Using Powder Materials to Replace Air-Gaps for Fringing Flux Reduction

Paul Winkler, Acal BFi Germany GmbH, Germany, paul.winkler@acalbfi.com
Wulf Günther, Acal BFi Germany GmbH, Germany, wulf.guenther@acalbfi.com

Abstract

Amorphous or nanocrystalline gapped cores as well as powder cores are both popular in industrial power choke design. Both show different advantages and drawbacks, depending on their function within a circuit. In this paper we present a design-approach, combining both core-materials for choke design. The drawbacks of air gapped solutions are shown and compared to a solution, where the air gap is replaced by a distributed gap using a piece of powder material. We illustrate the much higher fringing flux of an air gapped structure and related losses. The design procedure of an inductor using a powdered material instead of an air-gap and the different saturation behavior of both solutions are shown.

1. Introduction

For power-inductors, which are mainly storage chokes working at nominal currents in a range of 50-200 A and a frequency between 3-100 kHz, often gapped amorphous or nanocrystalline cores are used. They offer a much higher possible saturation flux density B_{sat} compared to ferrites (1,2...1,5 T instead of 0,3...0,4 T for ferrites), what makes them the preferred choice to build smaller inductors.
To store a high amount of energy, power-inductors build from amorphous or nanocrystalline materials require a relative large air gap, in the range of 2...10 mm. Fringing flux, entering the space around a big air gap, is problematic, due to forced eddy current losses [1, 2]. Ways to overcome this problem are the usage of multiple small air gaps, what causes a larger manufacturing effort, or the usage of lower-permeability powder materials with a permeability μ_r of 10 to 26, inserted instead of an air gap, which is the approach shown in this paper.
While combining two materials to form a core without an air gap, both should have a usable flux density B_{use} in the same range. KoolMμ (Sendust) material has a soft saturation curve with a B_{sat} in the range of around 1 T [3]. The preferred range of B_{use} in amorphous and nanocrystalline cores is, due to core loss effects, also in the range up to 1 T .

2. Fringing Flux and Eddy Currents

Fringing flux appears at any kind of discontinuity within the core, like air gaps or edges. The following Figure illustrates the fringing flux entering the winding at an air gapped inductor with an E-core.
Where the flux lines are entering the windings with high intense, strong electric fields $\vec{E}$ are induced following Faradays law (Equation 1), which leads to high eddy current density $\vec{J_e}$ in the high conductive material of the windings, following Ohms law (Equation 2). [1]

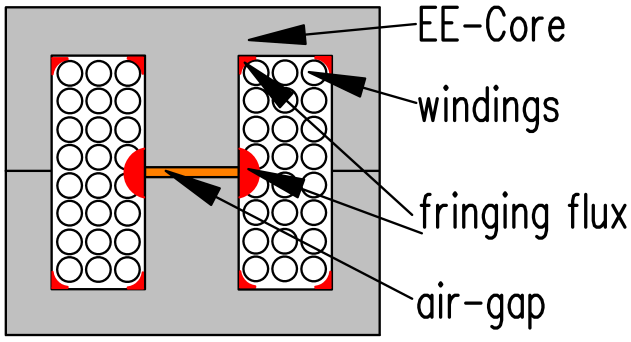

Fig. 1: Fringing Flux in an Air Gapped EE-Core

$$\nabla \times \vec{E} = -\frac{\partial B}{\partial t} \tag{1}$$

$$\vec{J_e} = \frac{\vec{E}}{\rho} \tag{2}$$

The eddy currents and so the losses around the air gap due to fringing flux are proportional to the level

ISBN 978-3-8007-4424-4

of the magnetic flux density B and its frequency (Equation 1). These losses can lead to hot spots inside the winding and the choke, having a negative impact on the electrical behavior and life-time. To avoid them, by a rule of thumb, a space between the windings and the core at the air gap should be twice the gap size. For larger air-gaps this value has to be increased significantly as the fringing flux effect increases as well, what reduces the space for the winding [1]. If laminated cores (like amorphous or nanocrystalline iron) are used, higher eddy current are also induced there, as the direction of the fringing flux is orthogonal and not parallel to the isolated laminations, when it is leaving or entering the core (Figure 2).

3. Reducing Fringing Flux Using Powder Material

In this section we compare the flux density around an air gap to the flux density around a KoolMμ block with the permeability of μ_{ini}=26, which is used as magnetic resistor instead of the air gap. Both designs end up having the same A_L value at the operation point (same excitation applied) and so form the same inductance in the overall core. They are shown in the following Figures 2 and 3. The soft magnetic material, the gap is placed in, is a amorphous iron based material with B_{sat}=1,5 T.

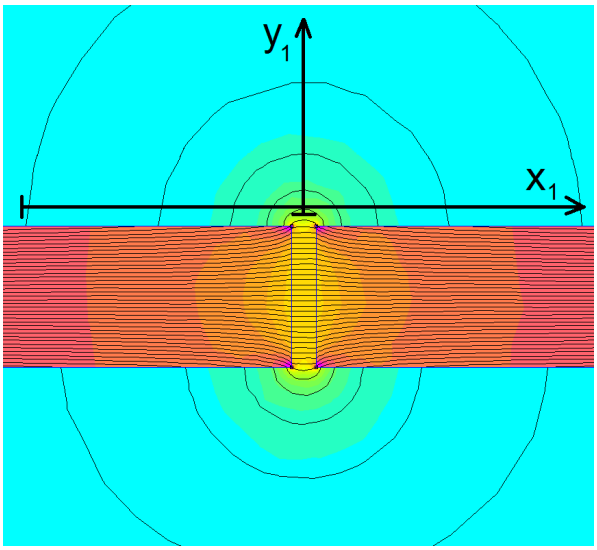

Fig. 2: Fluy Density at an Air Gap in an amorphous core

The flux density inside the Kool My block is around

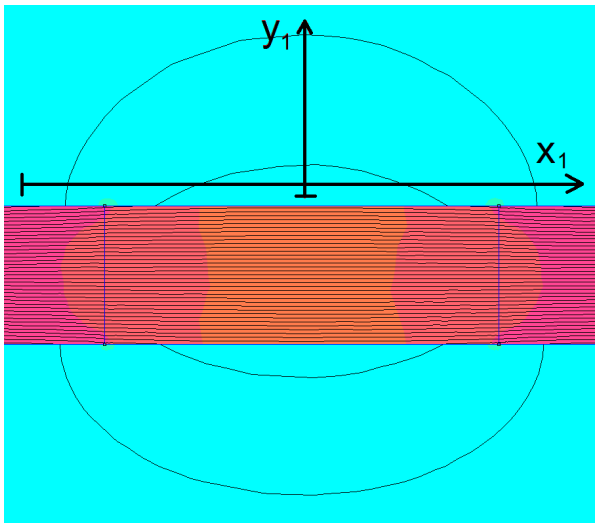

Fig. 3: Fluy Density at a KoolMμ piece in an amorphous core

400 mT, calculated with a finite element computation. At this level of flux both gap structures have the same magnetic resistance. They are excited with the same magnetomotive force Θ. How to calculate the length of a piece of powder material to replace an air gap, concerning its soft saturation curve, is discussed in section 4.
In both pictures two axes x_1 and y_1 are shown. They refer to the axes in the diagrams in Figure 4 and Figure 5, which show the total flux density along these traces.

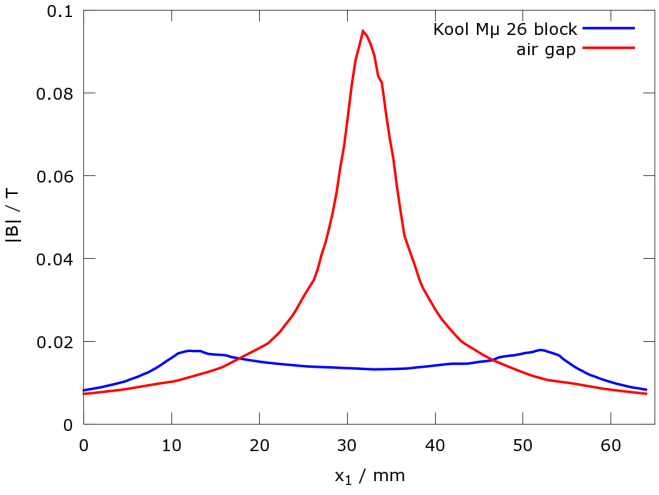

Fig. 4: Total Flux Density Along the Horizontal Trace x_1

The path x_1 has a distance in the range of the size of the air gap size from the core. Figure 4 illus-

trates the peak flux density in this distance of the air gapped structure to be approximately 5 times higher than using the KoolMμ block. The diagram

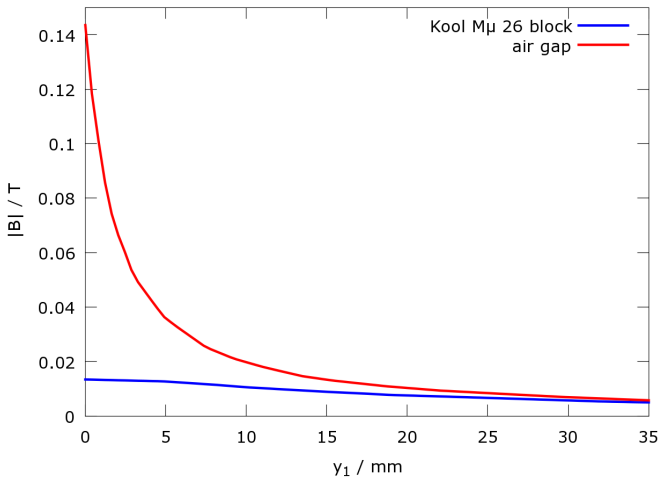

Fig. 5: Total Flux Density Along the Vertical Trace y_1

in Figure 5 shows the penetration of the room orthogonal to the air gap. Up to a distance of 15mm, which is 6 times the size of the air gap, the fringing flux at the air gap is significant higher (>1.5 times) than in the simulation with the KoolMμ block.

4. Analytical Calculation of Powder Material Block Size

In this section we show the calculation of the length of a powder core block to replace the air gap within an amorphous or nanocrystalline material.
As both amorphous and nanocrystalline iron cores have a much higher permeability (μ_{Fe} >8.000), the designer can assume that the whole magnetomotive force Θ is applied on the powder material (as it would be on the air gap). This is the case as long as the flux density in the iron material is not in the rang of the saturation fluy density B_{sat}, as than also inside the iron the permeability drops significantly.
Powder materials have, due to their structure, a soft saturation behavior, which is described as a function of the applied magnetic field (Equation 3). It shows the relation of their effective permeability μ_{eff} to their initial permeability μ_{ini} and is given by the powder core manufacturer [4, 5].

$$\frac{\mu_{eff}}{\mu_{ini}} = f(H) \tag{3}$$

The H-field in the powdered block equals to (assuming $\mu_{Fe} >> \mu_{powder}$):

$$H = \frac{\Theta}{l_{powder}} = \frac{N \cdot I}{l_{powder}} \tag{4}$$

Where N is the number of turns, I is the nominal current and l_{powder} the effective (average) path length of the magnetic flux inside the powdered material.
To approximate the right length of a block of power material to replace an air gap inside a choke, we start at a length, which is calculated using the initial (no load) permeability μ_{ini} of the powder material and the air gap length to replace l_{air}. Then Equations 3 and 4 are applied several times iteratively, until the length l_{powder} does not change anymore, see the following pseudocode.

$\mu_{eff} = \mu_{ini}$
$l_{powder} = l_{air}$
$l_{final} = 0$
while $l_{powder} \neq l_{final}$ **do**
  $l_{powder} = \mu_{eff} \cdot l_{air}$
  $H = N \cdot I / l_{powder}$
  $\mu_{eff} = f(H) \cdot \mu_{ini}$
  $l_{final} = \mu_{eff} \cdot l_{air}$
end

Algorithm 1: Iterative calculation of powder block length

When using the above shown analytical way to calculate the length of the powder block, following issues have to be considered:

- Unlike an air gap the permeability of the powdered material is not only influenced by saturation but also by temperature, mechanical stress and operation frequency. This eventually has to be considered in the above shown algorithm.
- In reality the effective permeability μ_{eff} and so the resulting l_{final} are smaller than the analytical calculated values. This is due less fringing flux and a higher percentage of flux inside the powder core compared to the air-gap solution, which results in a higher saturation in the powdered material. To detect the fitting length a Finite Element Method analyses or the construction of a prototype using

ISBN 978-3-8007-4424-4

several small powder material slides can be used.

- Equation 3 is a fitting-function, which does not work in high saturation cases

5. Design Example

5.1. Air Gapped Nanocrystalline Choke

In this section we show at a concrete example how an air gap is replaced by a piece of powder core (in this case a KoolMμ block). It is demonstrated, how the fringing flux, entering the space around the air gap and so the winding, is reduced.
The storage choke works on a DC current of I_n =48 A with an 20 kHz ripple of ΔI_{pp} =12 A as shown in the following curve. Its inductance is 290 μH until it starts saturating. Following the analytical calculation the saturation will be reached at around I_{sat} =100 A, which corresponds to a flux density of 1.2 T, reached in the biggest part of the iron material. Analyzing the saturation behavior of the complete choke numerically with FEMM will lead to the DC-saturation curve shown in Figure 13.

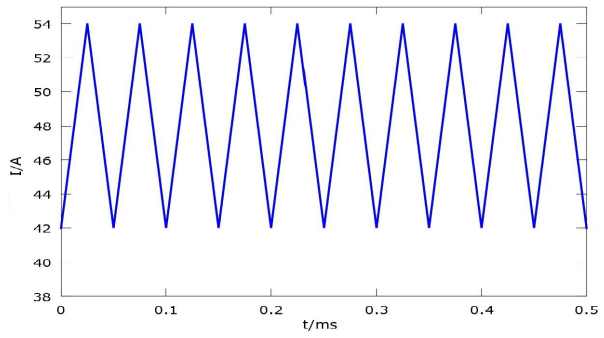

Fig. 6: Current Signal Through Inductor

The choke is constructed with a nanocrystalline core. Its cross-section is shown in Figure 7. The hight of the core is 35 mm. The magnetic path in this design contains two equal air gaps. Each has a length of 3.5 mm. The 44 turns are wound by 6 parallel strands of copper wire with 1.5 mm diameter, as shown in Figure 7.

In this design the distance of the winding from the core is 3.5 mm. During normal operation the nominal flux density B_n in the nanocrystalline Iron is at 0.54 T. The AC current forces a ΔB of 0,13T.

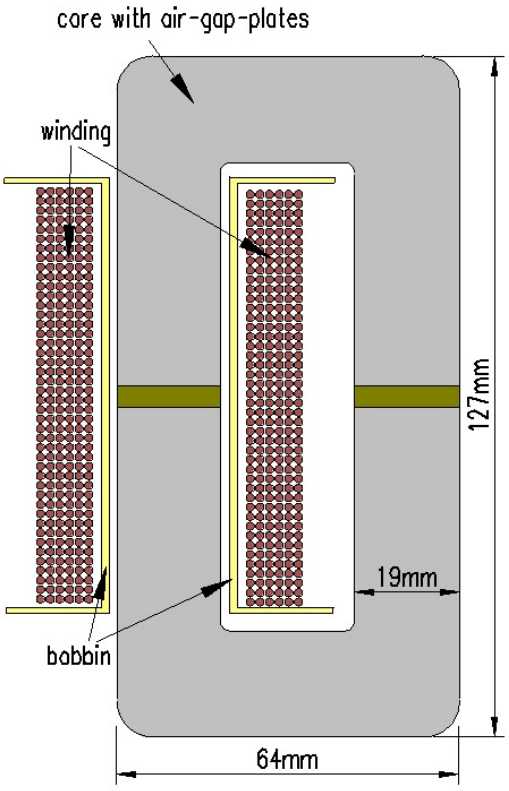

Fig. 7: Air Gapped Choke Cross Section

5.2. Replacement with KoolMμ 26

Both air gaps are replaced by a block of KoolMμ powder material with a initial permeability of μ_{ini} =26. The drop of the initial permeability of this material due to an applied DC current is shown in the following Figure [4].

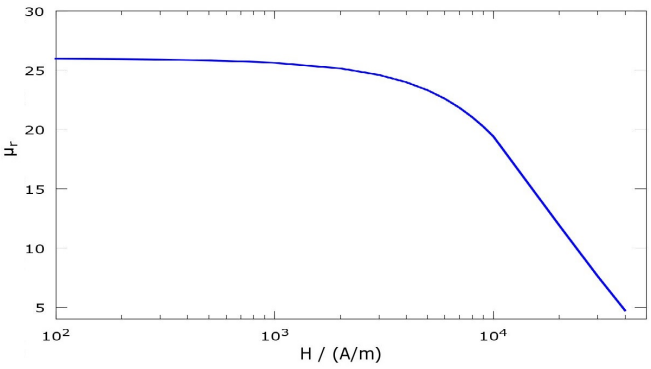

Fig. 8: Saturation of KoolMμ26

Using the Algorithm 1 and Equation 3 we receive the total powder length of 127 mm. So both KoolMμ blocks, replacing the air gaps, have a length of 63.5

mm. The nanocrystalline iron cut core has to become smaller, what is no problem due to its fabrication procedure. The complete design with its flux density plot is shown in Figure 9. It shows the overall design to have the same size as the solution with the air gaps, shown in Figure 7 and 10.

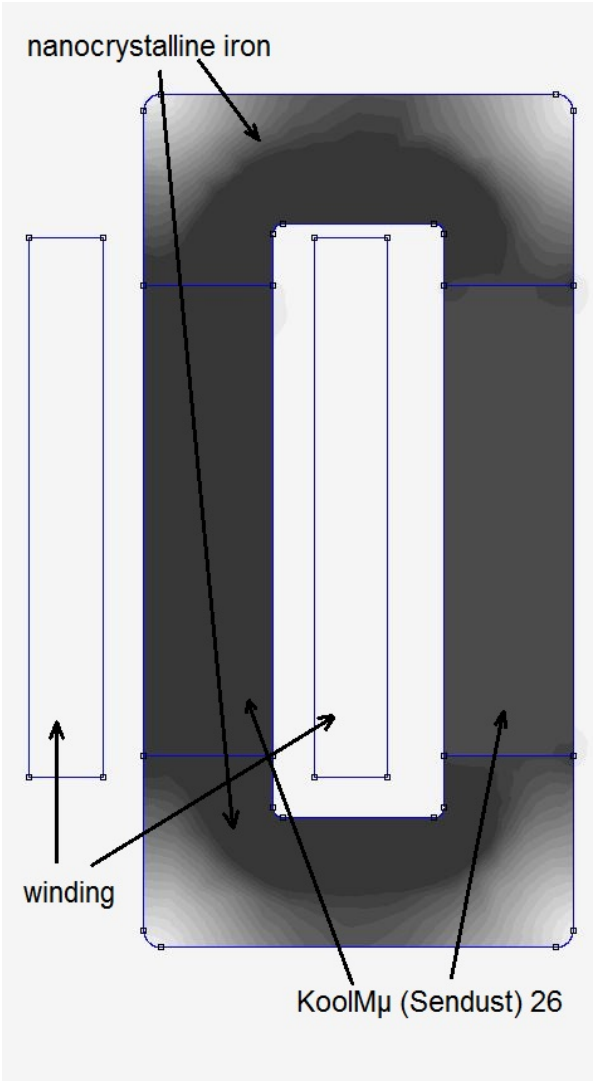

Fig. 9: Choke Flux Density using KoolMμ

The maximum flux density in Figure 9, shown as black colored area, is 0.54 T.

5.3. Comparisson of Both Designs

The flux density of both designs, when excited with the nominal current (48 A) is shown in the Figures 9 and 10. Using the same gray scale in both figures it is clearly shown, that the air gap makes the flux fringing around it and penetrating the winding. Using the KoolMμ powder pieces, the flux is forced to stay inside the core material and the fringing effect is reduced significantly.

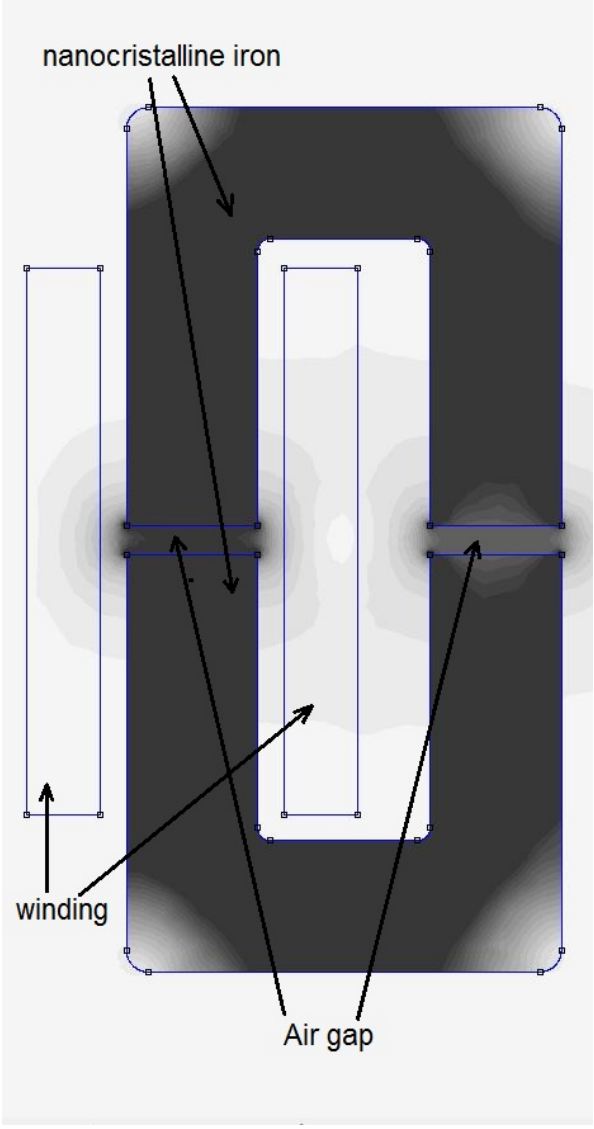

Fig. 10: Choke Flux Density using Air Gap

Like the DC-flux also the AC-flux, forced by the alternating current shown in Figure 6, is fringing at the air gap. The part of the alternating flux penetrating the winding will force high frequent eddy currents in high conductive parts like the winding. This will lead to losses and hot spots at the winding next to the air gap. With the design, where the air gap is replaced by a block of KoolMμ powder material, these losses and the local temperature rise are eliminated.

The AC-flux density along parallel traces in a distance of 2, 4, 6 and 8 mm from the left leg of the

ISBN 978-3-8007-4424-4

cores, shown in the Figures 9 and 10 was numerically calculated using FEMM. The AC-flux density of the outside of the core (left direction of left leg) is shown in Figure 11. The flux in the same distance from the core, but inside the winding window (right direction from the left leg) is shown in Figure 12. In both figures it is well illustrated that the fringing effect at the air gap is multiple times higher compared to the solution, which combines the nanocristalline cut core with the powder material. In this example, even in a large distance above 8 mm from the air gap the fringing flux is significant higher.

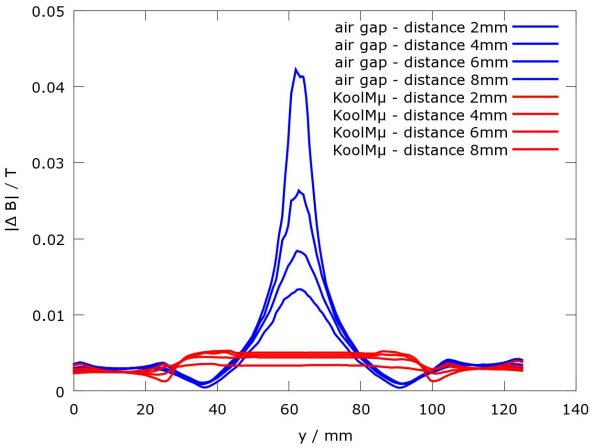

Fig. 11: AC-Flux Density at the Outer Core Side

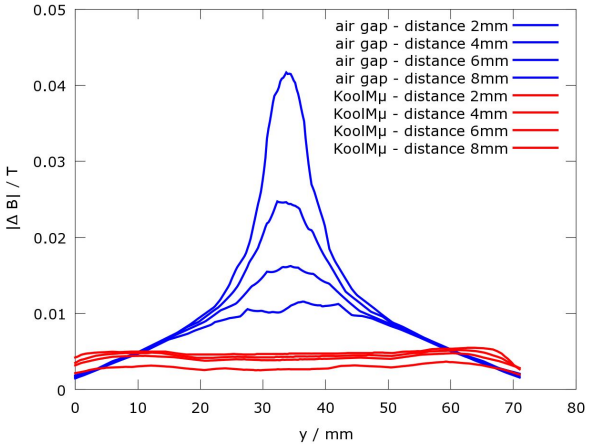

Fig. 12: AC-Flux Density in the Winding Window

As stated above, both designs result in chokes with the same size and shape. Both have the same number of turns and winding size. Due to the different construction of the core the two chokes show a different DC behavior (Figure 13). The solution with the powder block starts at a high no load inductivity and shows the typical soft saturation curve of powdered material, while the design with the air gap core has a constant inductivity up to its saturation point at around 100 A. The inductivity in the operation area is for both chokes at 290 μH.

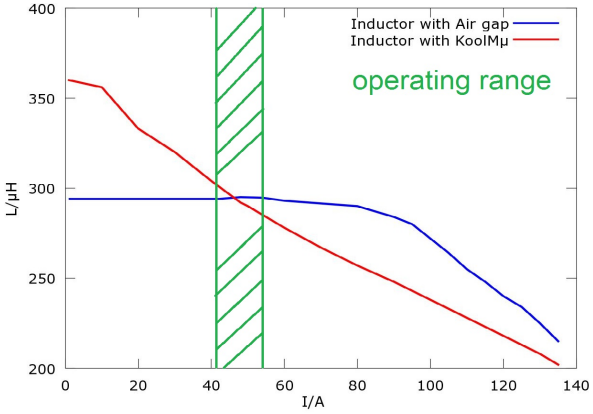

Fig. 13: Saturation Curve Comparison

6. Summary

In this paper we presented the approach to combine iron based cut cores with powdered materials to avoid fringing flux and its negative effects. Using the presented design approach enables the designer also to build smaller inductors, as a large distance between the air gapped core and the winding is not required, if the air gap is replaced with powdered material.
On a concrete example we demonstrate the replacement of an air gap leading to a core combined of KoolMμ blocks and nanocrystalline iron. Design hints are given and the different DC-behaviour of both chokes is shown.

7. References

[1] M. K. Kazimierczuk. *High-Frequency Magnetic Components*. Wiley, 2. edition, 2014.

[2] C. Wm. T. McLyman. *Transformer and Inductor Design Handbook*. CRC Press, 4. edition, 2011.

[3] M. A. Swihart. Inductor cores material and shape choices. Technical report, Magnetics.

[4] Magnetics. POWDER CORES. Catalogue, 2015.

[5] Micrometals. Power conversion & line filter applications. Catalogue, 2007.